



## Thermal-Hydrodynamic Simulation of Unsteady Drilling Fluid Intrusion and Mud Cake Evolution in Porous Reservoirs Based on CFD

Cuilong Kong<sup>1,2</sup>, Junliang Li<sup>2</sup>, Peng Wang<sup>2</sup>, Nan Zhang<sup>2</sup>, Shangyu Yang<sup>3</sup>, Fuping Feng<sup>1</sup>,  
Donglin Yang<sup>1\*</sup>

<sup>1</sup> Key Laboratory of Improving Oil and Gas Recovery, Ministry of Education, Northeast Petroleum University, Daqing 163318, China

<sup>2</sup> Daqing Oilfield Oil Recovery Technology Research Institute, Daqing 163318, China

<sup>3</sup> CNPC Tubular Goods Research Institute, Xi'an 710077, China

Corresponding Author Email: [nepu\\_ydl8082@126.com](mailto:nepu_ydl8082@126.com)

Copyright: ©2024 The authors. This article is published by IETA and is licensed under the CC BY 4.0 license (<http://creativecommons.org/licenses/by/4.0/>).

<https://doi.org/10.18280/ijht.430411>

### ABSTRACT

**Received:** 19 February 2025

**Revised:** 8 July 2025

**Accepted:** 28 July 2025

**Available online:** 31 August 2025

#### **Keywords:**

*reservoir permeability, drilling fluid intrusion, porous media flow, dynamic mud cake, permeability heterogeneity, numerical simulation*

The unsteady intrusion behavior of drilling fluid in permeable reservoirs plays a critical role in both wellbore stability and reservoir protection. To better understand the coupled thermal and fluid dynamic effects during this process, a porous medium seepage model is developed based on CFD, incorporating thermal effects to simulate transient temperature-sensitive infiltration behavior. A time-varying dynamic mud cake model is introduced as a boundary condition to reflect the evolving interface resistance, enabling fully coupled thermal-hydrodynamic simulations. The study compares three conditions—no mud cake, static mud cake, and dynamic mud cake—under varying reservoir permeability and thermal conductivity, systematically analyzing the influence mechanisms of mud cake on both fluid invasion depth and heat distribution. Results show that in high-permeability reservoirs, the mud cake significantly restricts early-stage intrusion of drilling fluid and delays heat penetration into the formation, but its control effectiveness weakens over time as the thermal gradient and pressure distribution evolve. In contrast, in ultra-low permeability formations, the presence of a mud cake has negligible impact on final intrusion depth or thermal propagation. The simulation quantifies the time-dependent evolution of both fluid and heat penetration under different operating conditions, and constructs a thermal-adaptive working map of mud cake applicability across various reservoir types. These findings offer theoretical insight and engineering reference for evaluating drilling fluid intrusion behavior and thermal effects in complex geological environments, particularly under high-temperature, deep-reservoir conditions.

## 1. INTRODUCTION

During the drilling process, the positive pressure difference between the drilling fluid column and the formation pore pressure leads to the continuous invasion of drilling fluid into the surrounding porous reservoir formations [1, 2]. As this fluid intrudes, suspended solid particles in the drilling fluid deposit onto the wellbore surface, gradually forming a low-permeability mud cake layer. This mud cake plays a pivotal role in regulating both hydraulic and thermal behaviors at the fluid-formation interface. Its formation and structural evolution exert a critical influence not only on the penetration depth of the fluid but also on the associated heat transfer mechanisms. The permeability of the formation directly impacts both the extent of fluid intrusion and the properties of the mud cake itself [3, 4]. In high-permeability formations, rapid mud cake development results in a compact structure that restricts both fluid flow and thermal migration. In contrast, low-permeability formations hinder effective particle deposition, leading to a loosely structured mud cake with limited capacity to obstruct intrusion or modulate thermal

exchange. This divergence highlights the need for a systematic investigation into the interplay between mud cake evolution, multiphase seepage, and heat transfer dynamics in varying geological settings.

To date, predictions of drilling fluid intrusion depth have been approached primarily through physical simulation and numerical modeling. Traditional filtration experiments, such as API filtration loss tests, are based on static or steady-state assumptions. While these offer operational guidance, they fail to capture the inherently transient, heat-sensitive nature of downhole fluid behavior. In reality, drilling fluid invasion is a multiphase and unsteady process where thermal effects and flow dynamics co-evolve. The temperature gradient between the high-temperature formation and the comparatively cooler drilling fluid alters viscosity, permeability, and local pressure distribution, thereby influencing fluid penetration. Moreover, the deposition and compaction of solids continuously modify both the hydraulic and thermal conductivities near the wellbore, forming a dynamic boundary layer with evolving thermophysical properties.

Some researchers have addressed these complexities

through innovative experimental designs. For example, a radial sand disk model was developed to visualize resistivity changes during multiphase intrusion [5], while others have constructed core-holder systems with integrated pressure and temperature controls to simulate coupled filtration under realistic wellbore conditions [6, 7]. These setups have contributed to a better understanding of the evolving saturation and thermal profiles. On the numerical side, studies have shown that radial filtration loss correlates positively with exposure time and pressure differential, and negatively with fluid viscosity—factors all strongly influenced by temperature. Building on two-phase flow theory and ion diffusion principles, a predictive model was proposed that accounts for reservoir-specific characteristics under variable thermodynamic conditions [8].

Efforts to characterize dynamic mud cake formation have also advanced. Sharma et al. [9] introduced a filtration-based mathematical model using loss coefficients and formation damage indicators to characterize the interplay between invasion and near-wellbore alteration. More recent models integrate the conservation of mass and radial flow resistance to simulate the coupled movement of fluid and solids, with validation from laboratory tests such as API filtration and dynamic core plugging experiments [10]. The modeling landscape has progressed from one-dimensional linear approximations [11] to more comprehensive three-dimensional CFD frameworks [12]. However, many of these models simplify the process to single-phase flow and overlook the temperature-dependent behaviors of mud cake and drilling fluids. When fluid properties differ significantly or thermal effects dominate, single-phase assumptions lead to inaccuracies. Thus, two-phase flow models incorporating heat transport offer a more robust and realistic basis for predicting dynamic invasion behavior under varying reservoir and thermal conditions.

Despite these developments, several key issues remain unresolved. Notably, the formation mechanisms and structural features of mud cake vary significantly across reservoirs, and the impact of these variations on both fluid intrusion depth and local thermal field distribution is still not well understood. To address this, the present study constructs a CFD-based multiphase seepage model that couples fluid flow with the thermal and structural evolution of the mud cake. By incorporating time-dependent permeability and thickness parameters of the mud cake, and solving the two-phase Darcy flow equations alongside the conservation of energy and mass, this study simulates how mud cake development governs the depth and thermal spread of fluid invasion across formations of differing permeability. Comparative analysis of static and dynamic mud cake models under various geological and thermal conditions is performed to identify their respective domains of applicability and critical threshold behaviors. The results aim to enhance the accuracy of drilling fluid invasion prediction while offering a thermally informed framework for assessing near-wellbore formation damage and designing adaptive fluid strategies in complex, temperature-sensitive drilling environments.

## 2. DRILLING FLUID INTRUSION FORMATION MECHANISM

Figure 1 illustrates the driving forces behind drilling fluid invasion into the formation. As shown in the figure, the

hydrostatic pressure of the liquid column serves as the primary driving force for drilling fluid invasion into the formation. Drilling fluid intrusion is a complex physic-chemical process involving multi-scale seepage-mass transfer coupling, the essence of which is a dynamic non-equilibrium process driven by positive pressure differential in which the drilling fluid system displaces the pore fluid in the reservoir and gradually permeates deep into the formation. From the perspective of micro-dynamics, the process contains three intercoupled physical mechanisms: the displacement mainly occurs in the washing zone area near the well wall, and its osmodynamic behavior follows Darcy's law of two-phase seepage [13-16]; The mixing process is manifested as the process of intersolution mass transfer between the drilling fluid filtrate and the formation fluid, which is controlled by the fluid phase equilibrium relationship. Diffusion is driven by the chemical potential gradient, and its mass transfer rate obeys Fick's law of diffusion. During drilling fluid invasion, flow, diffusion, and mixing play distinct roles, with flow being overwhelmingly dominant. The high pressure differential often several megapascals drives rapid filtrate penetration through Darcy flow, exceeding diffusion rates by orders of magnitude. This flow-dominated process dictates the overall invasion profile. Diffusion, though always present, remains negligible under dynamic flow due to low chemical potential gradients and formation diffusion coefficients. It only becomes relevant in stagnant zones or after well shut-in.

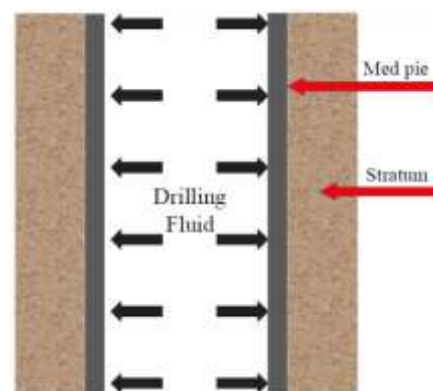


**Figure 1.** Schematic diagram of drilling fluid intrusion strata

Mixing is not a separate mechanism but emerges from the coupling of flow and diffusion: flow causes macroscopic fluid displacement and stretching, while diffusion slowly homogenizes compositions locally. Thus, the extent of mixing is primarily governed by the flow field. In summary, the invasion process is structured by flow, subtly modulated by diffusion, and expressed through mixing. These three mechanisms jointly determine the dynamic evolution characteristics of drilling fluid intrusion through spatio-temporal coupling. At the macroscopic seepage field scale, the intrusion of drilling fluid will form a typical radial zoning structure: the high displacement zone close to the well wall constitutes a flushing zone, the saturation of the primary fluid is significantly reduced, and the pore space is mainly occupied by the drilling fluid filtrate. The outward extension is a transition zone with continuous changes in fluid components, and its spatial distribution is controlled by the synergy of formation permeability anisotropy, pore structure heterogeneity and drilling engineering parameters. The outermost side is the undisturbed intact stratum that maintains the original fluid saturation and component distribution.

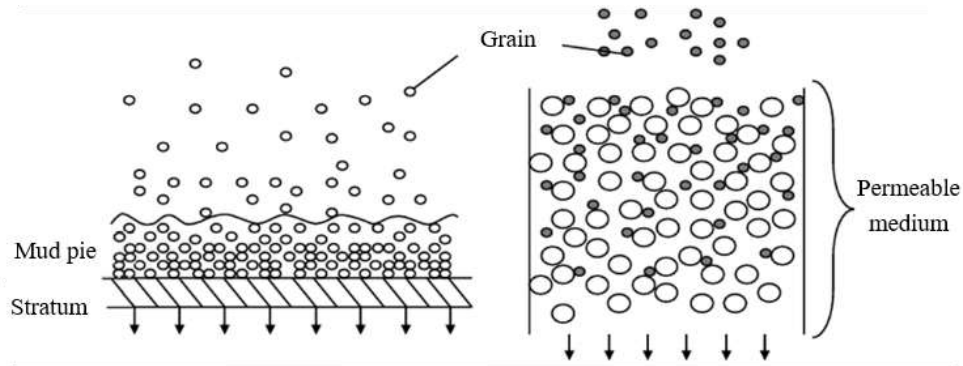


**Figure 2.** Schematic diagram of the formation mechanism of mud cake

The formation of mud cake on the well wall is due to the intrusion of liquid phase in the drilling fluid into the formation, while the solid phase particles gradually accumulate on the surface of the well wall. Figure 2 illustrates the mechanism of mudcake formation. When the suspension flows through the filtration medium, particle deposition occurs on the inner surface of the medium, resulting in the virtual absence or significantly reduced concentration of particles in the filtrate. Depending on the hydrodynamic conditions, the process can be divided into two typical modes: blind-end filtration and cross-flow filtration. Deep filtration mainly manifests the migration, adsorption and deposition behavior of submicron particles in the pores of the percolation medium.

Experimental studies show that when the median particle size is in the same order of magnitude as the average pore size of the medium, surface mud cake filtration plays a leading role. When the particle size is significantly smaller than the pore size of the medium, the deep filtration effect is more significant. Since solid-phase particles in drilling fluids usually have a wide particle size distribution range, the two filtration mechanisms often coexist and are coupled to each other [14-18]. In the initial stage, larger particle size particles preferentially bridge the surface of the medium to form the initial mud cake, while nanoscale particles penetrate into the deep layer of the medium. As the filtration process continues, the formed mud cake layer will participate in the subsequent particle separation process as a new functional filter medium due to its unique secondary pore structure. Numerous studies have demonstrated that incorporating nanoparticles [17] into drilling fluids significantly enhances the microstructure of mudcakes. By filling mudcake pores, reducing average pore size, and forming a denser network structure, nanoparticles substantially improve the mudcake's sealing capacity. This enhancement directly influences the core seepage process examined in this study. On one hand, the denser mudcake greatly reduces the dynamic filtration rate of drilling fluid filtrate, weakening the pressure-driven flow between the wellbore and the formation, thereby fundamentally mitigating both the intensity of filtrate invasion and its depth. On the other hand, the reduction in total invaded filtrate volume and flow rate indirectly affects subsequent mixing and diffusion processes: not only is the macroscopic mixing scale between filtrate and formation fluids limited, but the decreased flow rate also reduces the local Péclet number, increasing the relative significance of chemical potential-driven molecular diffusion in local regions. Thus, through the key mechanism of optimizing mudcake quality, nanoparticle addition exerts a systematic influence on the entire dynamic process of drilling fluid invasion. It enhances the barrier function of the mudcake, suppresses pressure-driven forced seepage, and consequently

reshapes the relative importance of seepage, diffusion, and mixing. This dynamic dual filtration mechanism not only significantly affects the spatiotemporal distribution characteristics of drilling fluid filtration loss, but also has a decisive impact on the quality of the final mud cake.

### 3. DRILLING FLUID INTRUSION FORMATION MODEL UNDER DIFFERENT CIRCUMSTANCES

Since formation permeability plays an important role in the penetration depth of drilling fluid and the physical parameters of mud cake formation, this paper divides the common reservoirs into five types of reservoirs, including ultra-high permeability, high permeability, medium permeability, low permeability and ultra-low permeability, according to the conventional oil and gas reservoir classification standard and the permeability as the dividing condition, and the permeability range is shown in Table 1.

**Table 1.** Reservoir division criteria

Permeability Grade	Range (mD)
Extra-High Permeability	>2000
High Permeability	500~2000
Medium Permeability	50~500
Low Permeability	10~50
Extra-Low Permeability	1~10
Ultra-Low Permeability	1<

During the over-equilibrium drilling process, the drilling fluid invades the reservoir driven by the positive pressure difference, triggering the redistribution and migration of the oil-water phases in the near-well zone, forming a coupled two-phase seepage system composed of well bore, dynamic mud cake and reservoir. In order to accurately describe this dynamic process, a mathematical model needs to be established to couple the dynamic filtration loss of drilling fluid in the well bore with the seepage process of oil and water in the reservoir. Based on the actual physical mechanism, the model is based on the following basic assumptions: (1) there are only oil and water two-phase fluids in the reservoir; (2) The multiphase seepage in the strata around the well follows Darcy's law; (3) Ignore the influence of capillary force.

#### 3.1 Mathematical model of drilling fluid intrusion formation without considering mud cake conditions

In the theoretical modeling of drilling fluid intrusion into the formation, if the formation and influence of mud cake are

ignored, it can be assumed that the drilling fluid is always in direct contact with the well wall, and the effective pressure difference acting on the formation interface is constant, which is equal to the difference between the drilling fluid column pressure and the formation pore pressure. Under these conditions, the drilling fluid intrusion process can be simplified to single-phase seepage in the porous medium, and its flow behavior conforms to Darcy's law, which can be expressed as [18]:

$$V_1 = -\frac{K}{\mu} \nabla P$$

where, in  $V_1$  the Darcy penetration velocity, m/s;  $K$  is the formation permeability, mD;  $\mu$  is the dynamic viscosity of the fluid, Pa·s;  $\nabla P$  is the driving force, MPa.

Under the condition of ignoring the source sink term, the flow of drilling fluid in the porous medium follows the law of conservation of mass, and its continuity equation is:

$$\frac{\partial}{\partial t}(\phi_f \rho_1) + \nabla \cdot (\rho_1 V_1) = 0$$

where, in  $t$  time, s;  $\rho_1$  is the density of the fluid, kg/m<sup>3</sup>.

Substituting Darcy's law into the continuity equation gives the basic seepage differential equation describing pressure diffusion:

$$\frac{\partial}{\partial t}(\varepsilon_s \rho_1) = \nabla \cdot \frac{\rho_1 K}{\mu} (\nabla P)$$

For the multiphase seepage situation, the two-phase Daxi flow model is used to describe the interaction between drilling fluid and formation fluids (such as oil phase). The effective viscosity of each phase was characterized by the coupling of relative permeability and saturation. The mixture viscosity model can be expressed as [19]:

$$\bar{\mu} = \frac{\bar{\rho}}{\frac{k_{r1} \rho_1}{\mu_1} + \frac{k_{rw} \rho_w}{\mu_w}}$$

where, in  $k_{r1}$  relative permeability of oil;  $k_{rw}$  is the relative permeability of water;

Mixture equivalent viscosity model:

$$\frac{1}{\bar{\mu}} = S_1 \frac{k_{r1}}{\mu_1} + S_w \frac{k_{rw}}{\mu_w}$$

In the porous media multiphase flow module, the fluid volume fraction inside the porous medium lacks the relevant control conditions. For simulating the migration and diffusion of drilling fluid intrusion in porous media, the two-phase Darcy Law module has ideal and uniform results due to the control of relevant conditions [20].

$$S_1 + S_w = 1$$

where, in  $S_1$  integral number of drilling fluid;  $S_w$  is the oil volume fraction of the formation.

In this model, the system of control equations for Darcy's law of two phases can be written as:

$$\frac{\partial}{\partial t}(\phi_0 c_g) + \nabla \cdot \left( c_g \left( -\frac{K}{\mu} \nabla P \right) \right) = \nabla \cdot c_g$$

The initial conditions for the seepage field in the formation are defined by the original fluid pressure and saturation prior to drilling operations:

$$\begin{cases} P_w = P_{w0} \\ S_w = S_{w0} \end{cases}$$

Upon completion of drilling, the drilling fluid acts directly on the wellbore wall, where the internal pressure remains constant and equal to the wellbore pressure, while the fluid saturation also remains unchanged. Thus, the inner boundary condition of the formation is defined as:

$$\begin{cases} P_w = \nabla P \\ S_w = S_{wb} \end{cases}$$

For the outer boundary of the system, both the formation pressure and fluid saturation retain their original values. Therefore, the outer boundary condition of the formation is given by:

$$\begin{cases} P_w = P_{w0} \\ S_w = S_{w0} \end{cases}$$

### 3.2 Considering the drilling fluid intrusion formation model under mud cake conditions

Mud cake plays a key control role in the intrusion process of drilling fluid, and its formation is a dynamic evolution process accompanied by time-varying characteristics of porosity and permeability. The dynamic behavior of mud cake significantly affects the pressure distribution and filtration rate in the near well zone, which in turn affects the intrusion depth of drilling fluid and the degree of formation damage. During the filtration process, the porosity and permeability of the mud cake continued to change with time, and the permeability of the mud cake and the permeability of the thickness were affected. Therefore, it is very important to accurately characterize the intrusion depth of drilling fluid and the physical properties of the formation around the wellbore hole. The drilling mudcake prediction equation proposed by Zhao [21], as adopted in this study, derives its applicability from the underlying physical mechanisms of cross-flow filtration theory on which the model is based. The validity of this equation highly depends on the composition and stability of the drilling fluid system. Its core assumptions include a predictable particle size distribution and concentration of solid phases in the drilling fluid, as well as stability under shear, ensuring that particle deposition and compaction remain a mechanically-dominated process. As a result, the model demonstrates strong predictive performance for water-based or oil-based drilling fluids with sufficient solid content and stable properties. However, in formations rich in water-sensitive clay, physicochemical interactions such as hydration, swelling, and dispersion of the formation rocks may significantly interfere with the mechanically-dominated mudcake formation process. Under such conditions, additional modifications may be required to improve the predictive

accuracy of the model. Based on mass conservation and particle deposition kinetics, the equation for the thickness of the mud cake is:

$$L_{c(t)} = \sqrt{\left(k \frac{\Delta x_m}{k_m}\right)^2 + 2 \frac{\varepsilon_{so}}{\varepsilon_s - \varepsilon_{so}} \frac{k}{\mu} \Delta P \gamma t - k \frac{\Delta x_m}{k_m}}$$

where, in  $k$  is the permeability of mud cake,  $m^2$ ;  $\Delta x_m$  is the thickness of the percolation medium,  $m$ ;  $k_m$  is the permeability of the permeability of the permeate medium,  $m^2$ ;  $\varepsilon_{mo}$  is the solid phase content of drilling fluid;  $\varepsilon_s$  is the solid phase content of the mud cake;  $\mu$  is the viscosity of the liquid,  $Pa \cdot s$ ;  $\Delta P$  is the filtration loss pressure difference,  $Pa$ ;  $\gamma$  is the possibility of spherical particles deposited on the surface of the mud cake;  $t$  for time,  $s$ .

Dynamic permeability model:

$$k = (0.197\Delta P - 1.09)L_{c(t)} - 1.5v + 3.9$$

where, in:  $L_{c(t)}$  is the thickness of the mud cake,  $mm$ ;  $V$  is the viscosity of the drilling fluid,  $m/s$ ;

When the drilling fluid passes through the mud cake, there is a differential pressure loss, and when the drilling fluid touches the mud cake, the velocity equation at this time is:

$$V_1 = -\frac{K}{\mu} \nabla (P - P_s)$$

The subsequent calculation can be brought into continue to calculate the depth of drilling fluid intrusion into the formation after considering the mud cake. However, some scholars simply consider the introduction of mud cake as the fixed value after equilibrium, so this paper analyzes the dynamic mud cake stability value as the third case.

#### 4. MATHEMATICAL MODEL SOLUTION OF DRILLING FLUID INTRUSION STRATA

Figure 3 shows the established finite element numerical model. The white area represents the borehole, which is surrounded by the mud cake. The outermost layer is the virgin formation, the size of the simulated area of  $3\text{ m} \times 3\text{ m}$ . The model boundary is set to an impervious boundary to simulate a closed formation environment. The wellbore with a radius of  $0.1\text{ m}$  is set in the center, and the drilling fluid seeps and diffuses from the wellbore to the surrounding porous medium under the pressure of the liquid column. In order to accurately capture the distribution characteristics of drilling fluid filtrate in the near-well area, the radial grid is used to divide and locally encrypt the near-well area. Two fluids are considered in the model: phase 1 is the drilling fluid filtrate, and phase 2 is formation crude oil.

To evaluate the impact of grid number on numerical simulation results, a grid independence analysis was conducted in this study. As shown in Figure 4, the invasion depth of drilling fluid after two days was compared across six different grid configurations: 21,018; 5,9597; 24,240; 15,364; 12,708; and 6,722. The results indicate that the simulated invasion depth varies significantly when the grid number is below 24,240, but stabilizes once the grid count exceeds this value. Meanwhile, the computation time increases markedly

with higher grid numbers, with computational costs rising sharply beyond 24,240 grids. Therefore, considering both accuracy and efficiency, a grid number of 24,240 was selected for all subsequent numerical simulations in this study.

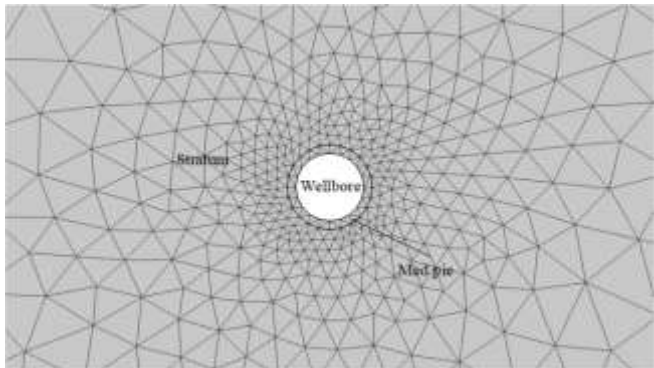


**Figure 3.** Finite element simulation of drilling fluid intrusion formation modeling

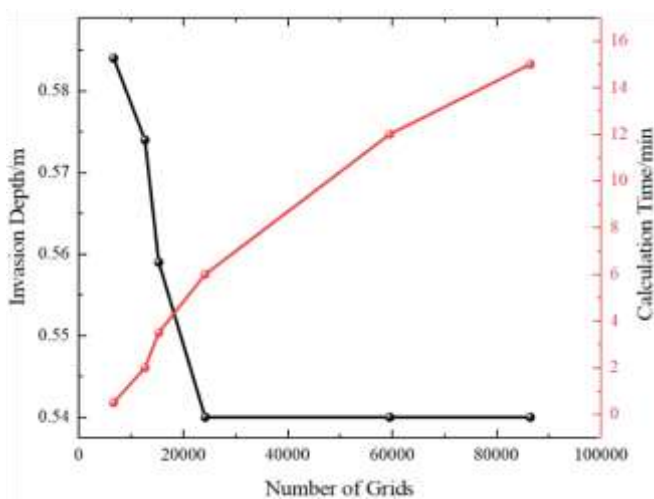
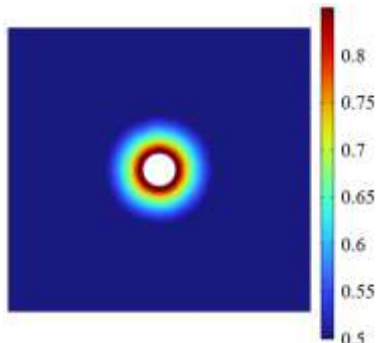


**Figure 4.** Computational results and computation time under different grid numbers

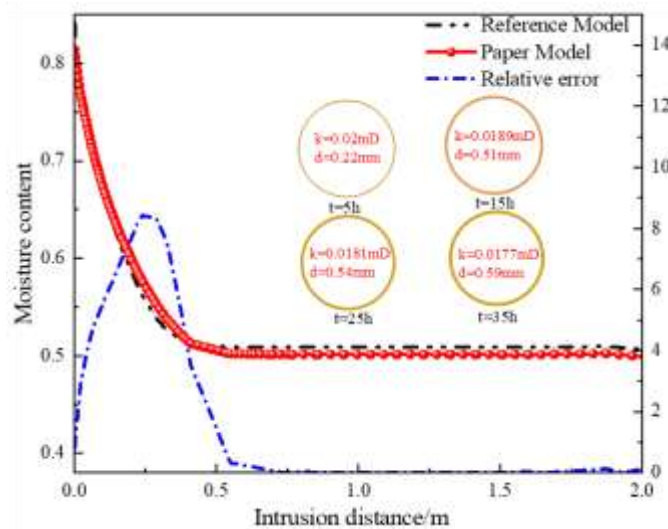
##### 4.1 Verification of drilling fluid intrusion formation model

To verify the accuracy of the model built. The calculation results of the dynamic mud cake proposed in this paper are compared with the models of Fan et al. [22] and other models to verify the accuracy of the distance of drilling fluid intrusion into the reservoir. The experimental parameters of stratigraphic module-scale rock samples were selected, with permeability of 30 mD, porosity of 20%, oil saturation of 80%, residual oil saturation of 50%, and differential pressure of 2 MPa.

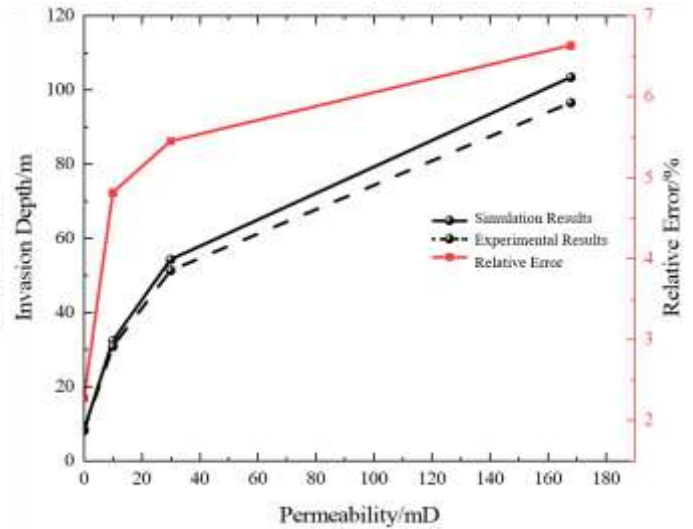


(a) Figures of numerical simulation results





(b) Model validation



(c) Invasion depth under different permeability conditions

**Figure 5.** Verification of dynamic mud cake thickness and permeability

Figure 5(b) presents the temporal validation of the Fan Yiren model. After applying the established mudcake mathematical model to finite element simulations, the average consistency between simulated and experimental values of dynamic mudcake thickness and permeability reached 96.69%, with corresponding relative errors of 3.31%. All error metrics were controlled within 10%, demonstrating the high computational accuracy of the proposed model.

Figure 5(c) shows simulation results under different permeability conditions [23-25]. It can be observed that as core permeability increases, the error gradually grows. This is attributed to the fact that high-permeability cores facilitate more pronounced mudcake formation, which under laboratory conditions is influenced by multiple factors [26, 27]. Nevertheless, despite the increasing trend in error with higher permeability, all errors remain within 10%, confirming the reliability of the numerical simulations.

#### 4.2 Analysis of drilling fluid intrusion formation law under different reservoir conditions

Under the condition that only the formation permeability is changed and other parameters are not changed, the changes of drilling fluid intrusion depth from ultra-low permeability reservoir to high permeability reservoir are simulated. The parameters of the mudcake were determined based on the measured field data from Zhao Jingyuan's original paper, which provided reference values and variable ranges. This enabled the investigation of the influence of mudcake properties on invasion depth across different reservoir types. The initial simulation parameters are shown in Table 2.

To differentiate the permeability of different reservoirs, the permeability of reservoirs from high-permeability to ultra-low-permeability was selected as 2000 mD, 1500 MD, 250 MD, 25 mD, 5 mD and 1 mD respectively.

Figures 6(a) to (f) compare the simulation results of drilling fluid intrusion under three working conditions: without mud cake, dynamic mud cake and static mud cake under different reservoir permeability conditions. Figure 7 illustrates the ultimate invasion depth of drilling fluid under various reservoir conditions. It can be seen from the figure that the time required for drilling fluid intrusion to reach dynamic equilibrium is significantly extended as the permeability of the

reservoir decreases. Taking the mud-cake-free model as an example (Figure 5(a)), when the permeability is 2000 mD, the intrusion process is completed quickly within 72 hours, and the maximum intrusion depth is 2.62 m, and then tends to be stable. In the ultra-low permeability reservoir (permeability 0.1 mD, Figure 5(c)), the intrusion process lasted up to 430 hours, with a final depth of only 0.05 m. This difference fully reflects the characteristics of low fluid seepage resistance and rapid pressure transfer in the hyperpermeable strata.

From the comparison of the three models, whether to consider the mud cake and its dynamic evolution in highly permeable reservoirs has a decisive impact on the simulation results. For example, at a permeability of 2000 mD (Figure 5(a)), the intrusion depth after 72 hours is 2.62 m without considering the mud cake, and the dynamic mud cake model is 1.75 m, compared with only 1.47 m for the static mud cake model. As a low-permeability boundary layer that evolved over time, the mud cake effectively inhibited the continuous intrusion of drilling fluid. If it is simplified to a fixed parameter (such as static mud cake), it will not reflect the dynamic behavior of gradually decreasing permeability and increasing thickness during its actual formation, resulting in a systematic underestimation of the intrusion depth. From the applicable conditions of the mud cake model, when the reservoir permeability exceeds 5 mD, the role of mud cake cannot be ignored. For example, in a 5 mD reservoir (Figure 6(e)), the intrusion depth difference between the mudcake-free model at 96 h is only 5%; But as penetration increased, the difference widened dramatically. This is due to the fact that low-permeability reservoirs exhibit extremely high flow resistance, which acts as a significant barrier. This barrier results in exceptionally low filtration rates and minimal filtrate flow, preventing solid particles in the drilling fluid from gaining sufficient transport energy or effective bridging space [28]. As a result, the formation of a continuous, dense, and effective sealing mudcake is hindered. The inherently low permeability of the formation itself provides a natural barrier that far exceeds the sealing effect of any artificially formed mudcake. The dominant flow resistance offered by the formation is several orders of magnitude higher than the additional resistance contributed by a potentially incomplete mudcake. Therefore, in such reservoirs, the flow dynamics and pressure propagation near the wellbore are primarily

controlled by the low-permeability nature of the formation. Given that the mudcake effect is negligible due to its ineffective formation and minimal impact, it can be reasonably disregarded within the allowable tolerance of engineering accuracy.

At 1500 mD (Figure 6(b)), the results of the two types of models differed by 23% at the same time. Especially in the strata with permeability higher than 100 mD, the dynamic mud cake effect is particularly significant. This is because the solid-phase particles in the drilling fluid under high permeability conditions are more likely to accumulate rapidly at the well wall, forming an unsteady filter cake layer with continuous changes in thickness and permeability, and the static assumption is no longer applicable.

Based on the results of the comparison of mud cake models under different reservoir conditions, in order to further quantify the influence of the dynamic behavior of mud cake on the intrusion simulation accuracy, a relative error map suitable for different time and permeability conditions is constructed. Figure 8 shows the relationship curve between reservoir permeability and drilling fluid intrusion depth

simulation error under multiple time nodes, and the matching relationship between the mud cake model and reservoir seepage characteristics can be systematically evaluated from the perspective of fluid dynamics [29].

Figure 8 shows the relative error relationship between the influence of mud cake in the drilling fluid intrusion depth model under different time conditions. It can be seen from the figure that when the ground layer permeability is low, the difference between the calculation results of the two models is small. This is mainly because the mud cake formed in the low permeability formation is thin and has a very low permeability, which has a limited hindrance effect on drilling fluid intrusion, so the intrusion depth predicted by the two models is relatively close. However, with the increase of formation permeability, the model without considering the mud cake will significantly overestimate the intrusion depth, resulting in a gradual increase in error. When the permeability reaches 2000 mD, the relative error can reach a maximum of 53.4%. The results show that in the highly permeable strata, the inhibitory effect of mud cake on filtrate intrusion is particularly significant, which must be fully considered in the actual process.

**Table 2.** Basic parameters of numerical simulation

Simulation Parameters	Number	Simulation Parameters	Number
Formation Permeability (mD)	1/5/25/250/1500/2000	Filter Loss Pressure Difference (MPa)	3
Formation Porosity (%)	12	Liquid Density (kg·m <sup>-3</sup> )	1200
Drilling Fluid Solid Content	0.04	Particle Density (kg·m <sup>-3</sup> )	3600
The Mud Cake Solid Content	0.25	Particle Diameter (m)	1.0×10 <sup>-5</sup>
Viscosity (Pa·s)	0.001	Drilling Time (d)	10
Maximum Protrusion Height (m)	4.98 × 10 <sup>-6</sup>	Bound Oil Saturation Density	0.3

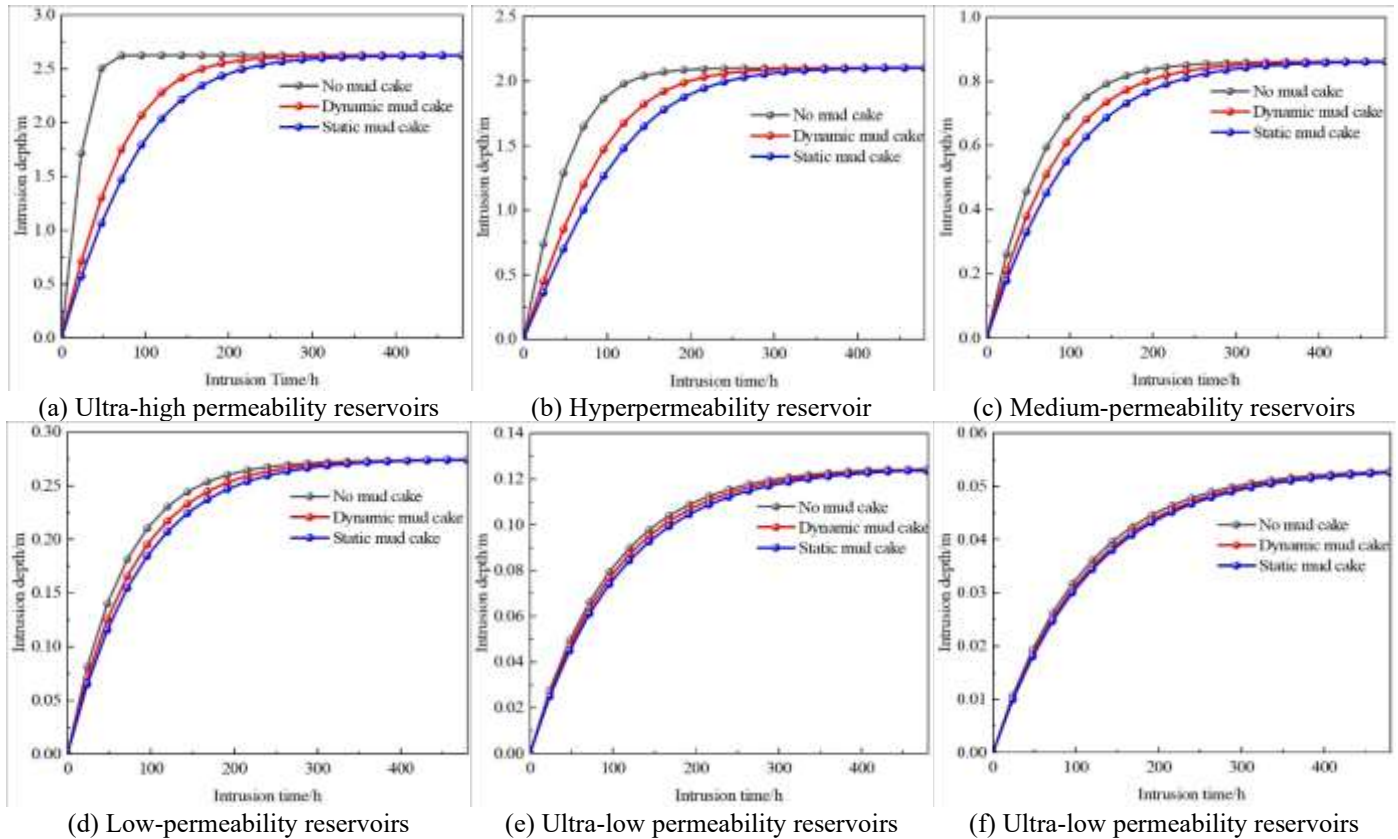


**Figure 6.** Results of mud cake drilling fluid intrusion under different conditions

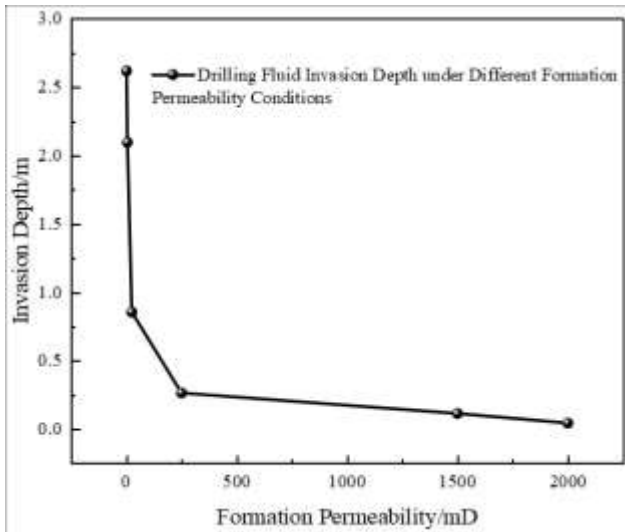


**Figure 7.** Drilling fluid invasion depth under different formation permeability conditions

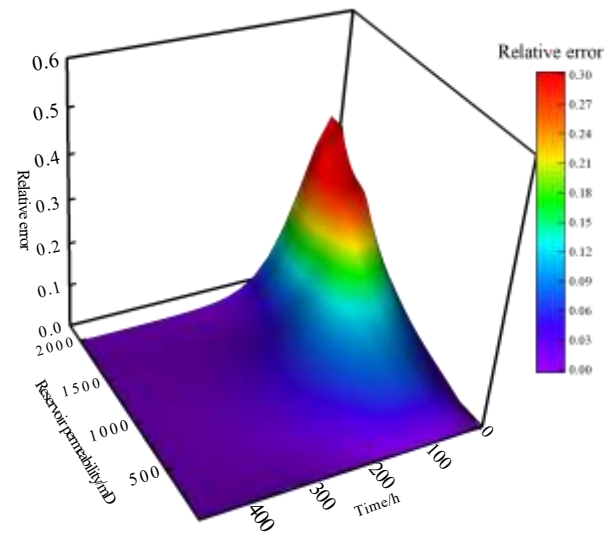


**Figure 8.** Diagram of relative errors

**Table 3.** Pattern of mud cake consideration under different reservoir conditions

Permeability Rate	Without Considering the Mud Cake	Consider the Mud Cake	Consider Dynamic Mud Cake
Extra-High Permeability	> 410 h	> 380 h	> 0 h
High Permeability	> 320 h	> 320 h	> 0
Medium Permeability	> 280	> 190 h	> 0 h
Low Permeability	> 150 h	> 80 h	> 0 h
Extra-Low Permeability	> 72h	> 48 h	> 0 h
Ultra-Low Permeability	> 0	/	/

Since the dynamic mudcake model most accurately represents actual downhole conditions during drilling fluid invasion, it is used as the benchmark for calculating the error values of the other two models (static mudcake and no mudcake). The formula is as follows:

$$W = -\frac{L_J}{L_D} \times 100\%$$

where,  $W$  is the error value;  $L_J$  is the invasion distance under static or no-mudcake conditions, in meters (m);  $L_D$  is the invasion distance under dynamic mudcake conditions, in meters (m).

According to Table 3, when the drilling time of the UHP reservoir reaches 410 hours, the intrusion depth of the drilling fluid tends to be maximized, and the influence of mud cake on the intrusion process can be ignored. With the decrease of reservoir permeability, the critical time of the mud cake effect can be gradually advanced without considering it. This is due to the thinner thickness and high permeability of the mud cake formed in the low-permeability reservoir, which significantly weakens the barrier effect on the intrusion of drilling fluid. When the reservoir permeability is less than 1 mD, the influence of mud cake is basically negligible, and the drilling fluid intrusion process can be simulated according to the mud cake-free model. In ultra-high-permeability reservoirs, mudcake's effect on invasion depth diminishes beyond 410 hours of drilling, allowing it to be ignored. Between 380–410 hours, the static mudcake model is recommended. During early phases (0–380 hours), the dynamic model must be used. As permeability decreases, the critical time for ignoring mudcake shortens—e.g., to 150 hours (no mudcake) or 80

hours (static mudcake) in low-permeability reservoirs. This is due to poor mudcake development: thinner layers, looser structure, and higher permeability reduce sealing efficiency. For reservoirs below 1 mD, mudcake impact is negligible, and invasion can be simulated without it. This study provides time-based criteria for model selection under varying permeability, improving simulation practicality.

## 5. CONCLUSION

Based on numerical simulation, the oil-water two-phase seepage equation and the dynamic mud cake equation are established, and the drilling fluid intrusion depth under different reservoir conditions and different mud cake methods is studied.

With the increasing permeability of reservoirs, the time point to reach the maximum distance of drilling fluid intrusion is constantly advanced, and the influence of mud cake on the intrusion distance also increases. When the reservoir permeability is 2000 mD, the drilling fluid penetration depth can reach 2.51 m, while when the reservoir permeability is 1 mD, the maximum intrusion depth is only 0.05 m.

When the permeability of the reservoir is greater than 1 mD, the influence of mud cake on the intrusion depth can be ignored. With the continuous increase of reservoir permeability, when the reservoir permeability is 2000 mD, when the time is greater than 410 h, the influence of mud cake can be ignored, and the time is in the range of 380 h~410 h, and the mud cake can be regarded as a static mud cake. while within 0~380 h, the impact of mud cake must be considered. When the permeability of the reservoir is reduced to less than 1 mD, the impact of the mud cake can be basically ignored,



and the distance of drilling fluid intrusion can only be considered as a non-mud cake.

However, the model presented in this study does not account for the coupling effect between the temperature field and the seepage field. During actual drilling operations, the temperature difference between the wellbore and the formation can induce thermal stress, alter fluid viscosity and phase equilibrium, and further affect filtrate invasion rates and mudcake deposition efficiency. Particularly in high-temperature and high-pressure reservoirs, this effect may significantly alter the invasion profile. Additionally, the model simplifies complex chemical interactions. Ion exchange, hydration reactions, and chemical precipitation between drilling fluid filtrate and formation fluids/rocks may modify pore-throat structures, wettability, and mudcake composition, thereby influencing its sealing performance. Neglecting these chemical processes could lead to an overestimation of sealing efficiency, especially in ultra-low-permeability reservoirs. Although these idealized assumptions help focus on the core physical mechanisms of seepage, they also imply that the current model is more suitable for reservoir environments with relatively inert chemical conditions and negligible thermo-pressure effects. Future work will integrate thermal-flow-chemical multi-field coupling theory to more comprehensively characterize the dynamic process of drilling fluid invasion.

## REFERENCES

- [1] Wang, Q., Wang, R., Sun, J., Sun, J., Lu, C., Lv, K., Qu, Y. (2021). Effect of drilling fluid invasion on natural gas hydrate near-well reservoirs drilling in a horizontal well. *Energies*, 14(21): 7075. <https://doi.org/10.3390/en14217075>
- [2] Feng, F.P., Wang, H.Y., Zhang, J.W., Han, X., Zhang, K. (2025). Mechanism of strength degradation of stratified shale under the action of drilling fluids. *Chinese Journal of Underground Space and Engineering*, 21(S1): 157-164.
- [3] Korsakova, N.K., Pen'kovskii, V.I. (2009). Phase distribution and intrapore salt exchange during drilling mud invasion of an oil-and gas-bearing formation. *Fluid Dynamics*, 44(2): 270-277. <https://doi.org/10.1134/S0015462809020112>
- [4] Akomolafe, F., El-Husseiny, A., Adebayo, A., Mahmoud, M., Bageri, B. (2025). A systematic investigation of drilling fluid bulk relaxation impact on NMR interpretation for formation evaluation. *Petroleum*, 11(3): 308-319. <https://doi.org/10.1016/j.petlm.2025.05.001>
- [5] Chen, F.X., Sun, J.X. (1996). Simulation test of radial electric conductivity during the mud filtrate invading porous formation. *Chinese Journal of Geophysics*, 39(S1): 371-378.
- [6] Hu, G.H., Yao, Y.J., Hu, Z.K., Zuo, X.Y. (1999). Experimental study on the influence of drilling fluid invasion on the electrical and physical properties of reservoirs. *Well Logging Technology*, 23(5): 323-326. <https://doi.org/10.3969/j.issn.1004-1338.1999.05.001>
- [7] Sun, Y.X., Li, C.L., Bai, X.S., Zhang, L.C., Zhao, J.Y., Guo, C.P. (2019). Study on factors affecting filtration property of drilling fluid with numerical simulation software. *Drilling Fluid & Completion Fluid*, 36(5): 581-586. <https://doi.org/10.3969/j.issn.1001-5620.2019.05.010>
- [8] Fan, Y.R., Hu, Y.Y., Li, H., Sun, Q.T., Chen, F. (2013). Numerical simulation of mud-cake dynamic formation and reservoir mud filtrate invasion. *Well Logging Technology*, 37(5): 466-471. <https://doi.org/10.3969/j.issn.1004-1338.2013.05.002>
- [9] Sharma, G., Tandon, A., Guria, C. (2025). An improved model for static filtration of water-based drilling fluids and determination of mud cake properties. *Fuel*, 393: 134882. <https://doi.org/10.1016/j.fuel.2025.134882>
- [10] Wang, J.H., Yan, J.N., Zheng, M., Feng, J., Feng, G.B. (2009). Prediction model for invasion depth of drilling fluid solid phase and filtrate into reservoir. *Acta Petrolei Sinica*, 30(6): 923-926. <https://doi.org/10.3321/j.issn:0253-2697.2009.06.022>
- [11] Windarto, Gunawan, A.Y., Sukarno, P., Soewono, E. (2012). Modelling of formation damage due to mud filtrate invasion in a radial flow system. *Journal of Petroleum Science and Engineering*, 100: 99-105. <https://doi.org/10.1016/j.petrol.2012.11.003>
- [12] Dong, L., Wu, N., Leonenko, Y., Wan, Y., Liao, H., Hu, G., Li, Y. (2023). A coupled thermal-hydraulic-mechanical model for drilling fluid invasion into hydrate-bearing sediments. *Energy*, 278: 127785. <https://doi.org/10.1016/j.energy.2023.127785>
- [13] Ibrahim, M.A., Jaafar, M.Z., Yusof, M.A.M., Chong, A.S., Idris, A.K., Yusof, S.R.M., Radzali, I. (2023). The effect of surface properties of silicon dioxide nanoparticle in drilling fluid on return permeability. *Geoenergy Science and Engineering*, 227: 211867. <https://doi.org/10.1016/j.geoen.2023.211867>
- [14] Akkutlu, I.Y., Yortsos, Y.C., Adagülü-Demirdal, G.D. (2010). Dual role of catalytic agents on in-situ combustion performance. *SPE Journal*, 15(1): 137-145. <https://doi.org/10.2118/115506-PA>
- [15] Ibrahim, M.A., Jaafar, M.Z., Yusof, M.A.M., Idris, A.K. (2022). A review on the effect of nanoparticle in drilling fluid on filtration and formation damage. *Journal of Petroleum Science and Engineering*, 217: 110922. <https://doi.org/10.1016/j.petrol.2022.110922>
- [16] Boaca, T. (2021). An identification problem related to mud filtrate invasion phenomenon during drilling operations. *Inverse Problems in Science and Engineering*, 29(12): 2401-2428. <https://doi.org/10.1080/17415977.2021.1914605>
- [17] Stamatakis, K., Tien, C. (1993). A simple model of cross-flow filtration based on particle adhesion. *AIChE Journal*, 39(8): 1292-1302. <https://doi.org/10.1002/aic.690390805>
- [18] Valle, B., Dal'Bó, P.F., Santos, J., Aguiar, L., Coelho, P., Favoreto, J., Borghi, L. (2021). A new method to improve the NMR log interpretation in drilling mud-invaded zones: A case study from the Brazilian Pre-salt. *Journal of Petroleum Science and Engineering*, 203: 108692. <https://doi.org/10.1016/j.petrol.2021.108692>
- [19] Boaca, T. (2021). Identification of the minimum value of reservoir permeability in nonlinear single phase mud filtrate invasion model. *Nonlinear Analysis: Real World Applications*, 59: 103274. <https://doi.org/10.1016/j.nonrwa.2020.103274>
- [20] Both, J.W., Cancès, C. (2025). A global existence result for weakly coupled two-phase poromechanics. *SIAM Journal on Mathematical Analysis*, 57(5): 4995-5038. <https://doi.org/10.1137/24M1688783>
- [21] Zhao, J.Y. (2021). Research on the damage law of aqueous phase trapping by cross-flow filtration of

- drilling fluid in tight gas reservoirs. Master's thesis, Northeast Petroleum University.
- [22] Fan, Y.R., Wang, X.L., Wu, Z.G., Wu, J.C., Jia, J.T. (2018). Simulation study on drilling fluid invasion considering formation damage. *Well Logging Technology*, 42(4): 383-389. <https://doi.org/10.16489/j.issn.1004-1338.2018.04.003>
- [23] Takahisa, H., Konno, Y., Jin, Y., Tenma, N. (2025). Effect of heterogeneous hydrate distribution on permeability: Pore filling hydrate presents high permeability. *Gas Science and Engineering*, 142: 205682. <https://doi.org/10.1016/j.jgsce.2025.205682>
- [24] Zhang, H.S., Cai, B., Liu, Y.B., Shi, X.C. (2017). Experimental study on drilling fluid invasion depth in tight sandstone of a certain block in the east China sea. *Journal of Southwest Petroleum University (Science & Technology Edition)*, 39(4): 152-158. <https://doi.org/10.11885/j.issn.1674-5086.2015.11.02.01>
- [25] Fan, Y.R., Wu, J.C., Wu, F., Zhou, C.C., Li, C.L. (2017). A new physical simulation system of drilling mud invasion in formation module. *Petroleum Exploration and Development*, 44(1): 125-129. [https://doi.org/10.1016/S1876-3804\(17\)30016-2](https://doi.org/10.1016/S1876-3804(17)30016-2)
- [26] Zhang, X.L. (2018). The evaluation method for the invasion depth of the filtrate of drilling fluids. *Guangdong Chemical Industry*, 45(9): 41-42. <https://doi.org/10.3969/j.issn.1007-1865.2018.09.018>
- [27] Debossam, J.G.S., de Freitas, M.M., de Souza, G., Amaral Souto, H.P. (2025). Numerical simulation of three-phase flow in petroleum reservoirs using a Picard–Newton sequential method. *Journal of the Brazilian Society of Mechanical Sciences and Engineering*, 47(7): 347. <https://doi.org/10.1007/s40430-025-05658-y>
- [28] Hedayati, E., Mohammadzadeh-Shirazi, M., Abbasi, A. (2025). Determining of fluid injection shear rate into the near wellbore region through the Computational Fluid Dynamics simulation. *Results in Engineering*, 26: 104733. <https://doi.org/10.1016/j.rineng.2025.104733>
- [29] Sypchenko, I.M., Afanasyev, A.A. (2024). Studying the effect of hysteresis of relative phase permeability on optimal strategies of water-gas impact on oil reservoirs. *Moscow University Mechanics Bulletin*, 79(2): 21-28. <https://doi.org/10.3103/S0027133024700043>